

Application of the Isolation Layer in Tunnel Crossing the Soft and Hard Rock Junction Subjected to Seismic Waves

Guangyao Cui¹⁾ and Jianfei Ma²⁾*

¹⁾ School of Civil Engineering, North China University of Technology, Beijing 100144, China.

²⁾ School of Civil Engineering, North China University of Technology, Beijing 100144, China.

* Corresponding Author: E-Mail: majfncut@163.com; ORCID: 0000-0003-2569-1656

ABSTRACT

Tunnels crossing the soft and hard rock junction suffer severe damages during strong earthquakes. In this paper, elastic-plastic numerical models considering the modified wave, the boundary condition and the monitoring system are established to investigate the seismic performance of the isolation layer in the soft and hard rock junction of the tunnel. The results show that tunnel safety is related to the proportion of soft and hard rocks, where the larger the proportion of soft rock is, the more vulnerable is the tunnel structure to the seismic waves. The maximum principal stress of secondary linings decreases by 50.23%-89.96%, 51.16%-98.95% and 55.98%-97.39%, respectively, when the dip angle of the soft and hard rock interface is 45°, 60° and 75° after the isolation layer is adopted. The seismic effects of the isolation layer with dip angles of 45°, 60° and 75° are 2.45%-121.67%, 13.19%-66.98% and 4.60%-131.83%, respectively. The application of the isolation layer significantly increases the safety of the tunnel crossing the soft and hard rock junction, except for the structure located at the soft-hard rock interface. It is suggested to adopt both isolation measures and structure reinforcements at the structure intersecting the soft and hard rock interface.

KEYWORDS: Tunnel engineering, Seismic response, Isolation layer, Seismic waves.

INTRODUCTION

Tunnel is a significant component of the transportation network. Its light damage may bring serious problems and huge losses to the traffic network. Traditionally, tunnels are believed to suffer minor seismic damage compared to the above-ground structure, because they are surrounded by soil or rocks (Dowding and Rozen, 1978). However, many severely damaged tunnels were observed in recent earthquake events (Tsinidis et al., 2020). The seismic damage databases and investigations of recent strong earthquakes have indicated that the tunnel portal section and the fault-crossing section are the most vulnerable parts of the mountain tunnel during strong earthquakes, including the 1995 Kobe, the 1999 Chi-Chi, the 2004 Niigataken-chuetsu, the 2008 Wenchuan and the 2016 Kumamoto earthquakes (Konagai et al., 2009; Li, 2012; Wang et al., 2001). In theory, the rock property is the

key factor that affects the seismic behaviors of mountain tunnels (Ismail et al., 2020). Compared with hard rock tunnel, the seismic damage of soft rock tunnel is more serious in earthquakes (Patil et al., 2018). The propagation effect of seismic force in soft rock is different from that in hard rock, so the seismic motion transmitted to the lining of hard rock tunnel and soft rock tunnel is also very different (Mayoral and Mosqueda, 2020). These discrepancies of seismic actions lead to serious damages to the tunnel structure at the junctions of soft and hard surrounding rock. In the 2008 Wenchuan earthquake, the soft and hard rock junctions of Jiujiaya Tunnel, Longxi Tunnel and Baiyunding Tunnel experienced severe seismic damages, such as lining cracking, water seepage and lining collapse, as shown in Fig.1(Cui et al., 2011). The seismic hazard in the junction of soft and hard surrounding rock of the tunnel has been classified as one of the typical seismic damages of mountain tunnels (Tsinidis et al., 2020). However, up to now, there are few studies on the seismic response of tunnels at the junction of soft and hard rocks.

Received on 3/1/2021.

Accepted for Publication on 3/3/2021.

Therefore, the seismic response and anti-seismic measures of the junction need to be further studied.

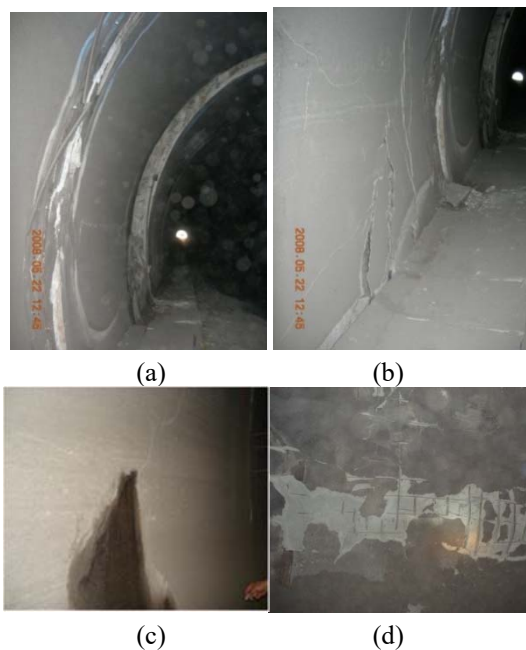


Figure (1): Seismic damages of soft-hard rock junction in Wenchuan Earthquake: (a) Staggered lining in Baiyundung tunnel; (b) Lining cracking in Baiyundung tunnel; (c) Inclined cracking and water seepage of lining in Ma'anishi Tunnel; (d) Lining spalling and block dropping in Youyi Tunnel

The earthquake damage of the tunnel is mainly determined by the deformation and displacement of surrounding rock. The vibration isolation and the structure reinforcement are the two most commonly used measures to reduce the displacement of tunnel surrounding rock to linings (Hashash et al., 2001; Konagai and Kim, 2001). Previous studies have shown that reinforcement methods, such as fiber concrete materials, rock bolting and rock grouting, have positive influences on the tunnel seismic performance, which are mainly realized by improving the strength and stiffness of the rocks or structures (Hassan et al., 2021; Jamshidi Avanaki et al., 2018). On the other hand, the isolation method was also proposed for tunnel seismic design (Shimamura et al., 1999). In many measures to block and absorb earthquake motion to the tunnel structure, the isolation layer is the most effective and simple way; that is, a layer of flexible material with high damping is used to wrap the lining structure of the tunnel from the

damage of earthquake motion (Suzuki et al., 2002). The existence of the flexible material layer makes the rock-lining system become the rock-layer-lining system. Also, the isolation layer prevents the seismic damage from the surrounding rocks to the lining structure (Kim and Konagai, 2000). Furthermore, the flexible layer reduces the intensity of the earthquake action and minimizes the pressure and the circumferential shear displacement between surrounding rock and secondary lining (Konagai and Kim, 2001). Therefore, in theory, the anti-seismic effect of the isolation layer is better than that of the structure reinforcement measures, especially in the weak parts of tunnels (Tsinidis et al., 2020; Zhao et al., 2018).

In general, the seismic absorption effect of the isolation layer is affected by numerous factors, such as tunnel shape, isolation layer materials, layer density and thickness, input motion... and so on. A lot of research has been done to explore the influence on the anti-seismic performance of the isolation layer (Chen et al., 2018; He et al., 2016; Ma et al., 2019). However, there are only a few studies that were conducted to investigate the isolation effect of the layer for the tunnel crossing the soft and hard rock junction. Therefore, in this paper, the numerical simulation method is used to study the seismic isolation effect of the isolation layer when the tunnel passes through the junction of soft and hard rock, as well as the influence of the inclination angle of soft and hard rock on the seismic isolation effect. Firstly, taking the Fanjiazhai Tunnel as a research background, finite difference models considering the modified waves, mechanical damping and monitoring system are established to study the seismic behavior of the tunnel crossing the soft and hard rock junction. The time history of the 2008 Wenchuan Earthquake wave is selected as the dynamic input for the numerical simulation, since the typical characteristics of the waves can well reflect the real responses in the project area. Secondly, the isolation layer is employed into the tunnel structure and the seismic effect of the isolation layer in the tunnel located in the soft and hard rock is analyzed. Finally, the models with the dip angle of the interface of 45° , 60° and 75° are developed to study the dip angle effect of the soft and hard rock on the seismic effect of the isolation layer and some scientific suggestions are given for the seismic design of the tunnel located in the soft and hard rock junction.

NUMERICAL ANALYSIS

Simulation Method

FLAC3D is an extended program of FLAC2D, which uses the mixed discretization procedure to simulate the yield and plastic flow characteristics of materials (Itasca Consulting Group, Inc., 2015). The mixed discretization procedure was proposed by scholars in the 1980s and its basic principle is similar to that of the discrete element method, but it can be used to solve continuous problems in irregular regions with various material modes and boundary conditions compared to the finite element method (Marti and Cundall, 1982). As a professional calculation program of geotechnical engineering, FLAC3D can not only calculate the stress and deformation states of engineering structures for three-dimensional rock mass, soil and other media, but also solve the problems of large deformation and failure of materials that cannot be solved by the general finite element method (Rinaldi and Urpi, 2020). In the process of solving, FLAC adopts the dynamic relaxation method of discrete element, which does not need to solve large simultaneous equations, so it is easy to realize on a microcomputer. The dynamic analysis module of FLAC adopts the explicit finite difference method, which can carry out three-dimensional complete dynamic analysis. In particular, the unique dynamic-multi-stepping method of FLAC3D can effectively reduce the calculation time of dynamic analysis (Esfeh and Kaynia, 2020). It is one of the most powerful tools to deal with nonlinear and dynamic problems. By defining the mechanical damping parameters, earthquake motion and boundary conditions in dynamic calculation, the seismic response of tunnel structures under earthquake can be accurately simulated.

Geological Condition

Fanjiashai Tunnel of Mangshi-liangjiahe expressway is 2468m long, which is an important component node of the expressway network in Yunnan Province of China. The tunnel site mainly passes through the complete, strongly and moderately weathered granulate. According to the relevant code of surrounding rock, the rock classes of completely and strongly weathered granulate are IV and V, respectively and those of moderately weathered granulate are III and IV (Ministry of Transport of the People's Republic of

China, 2004). The seismic fortification requirement of Fanjiashai Tunnel area is 8 degrees. The soft and hard rock junction of the numerical model is 1238m away from the tunnel portal and the dip angle of the interface is about 68-75 °. The lower part at the junction of soft and hard surrounding rock is moderately weathered granite with a grade of III, while the upper part is strongly weathered granulate with a grade of V. The support structure of the soft and hard rock junction of Fanjiashai Tunnel is a composite lining. The primary support is C20 shotcrete with a thickness of 0.30m and the secondary lining is C25 modeled concrete with a thickness of 0.50m (MOHURD, 2011). The lining model is shown in Fig. 2.

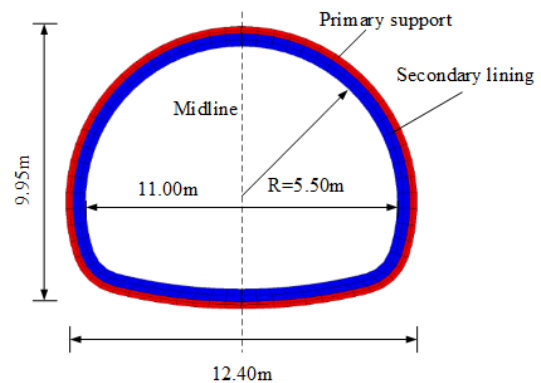


Figure (2): Support structure of Fanjiashai Tunnel

Numerical Model

The elastic-plastic model is established to simulate the seismic response of Fanjiashai Tunnel in soft and hard rock junction during strong earthquake. The Mohr-Coulomb model is adopted for rock materials, because the criterion could well reflect the real failure of rock mass. During the numerical calculation, it is assumed that the concretes of primary support and secondary lining in the tunnel structure are elastic materials. The depth of the tunnel is 50m and the longitudinal depth of the tunnel is 100m. In order to eliminate the boundary effect, the left-and-right width of the tunnel is 4 times the tunnel width, about 45m. The upper surrounding rock is soft rock with a class of V and the lower rock is hard rock with a rock class of III. The bedrock layer is 20m from the bottom of the model, which is the class II rock.

Test Cases

As the most commonly used isolation material in the tunnel engineering, sponge rubber plate with a thickness of 10cm is used as the isolation layer in this paper. In order to study the dip angle effect of the soft-hard interface on the seismic effect of the isolation layer, three control models without any seismic measures and three study models with isolation layers were established. The dip angles of the interface between soft and hard surrounding rock are 45°, 60° and 75°, respectively, as shown in Fig. 3. The isolation layer is applied between the surrounding rock and the secondary lining (see Fig. 4). Table 1 lists the test cases of this paper.

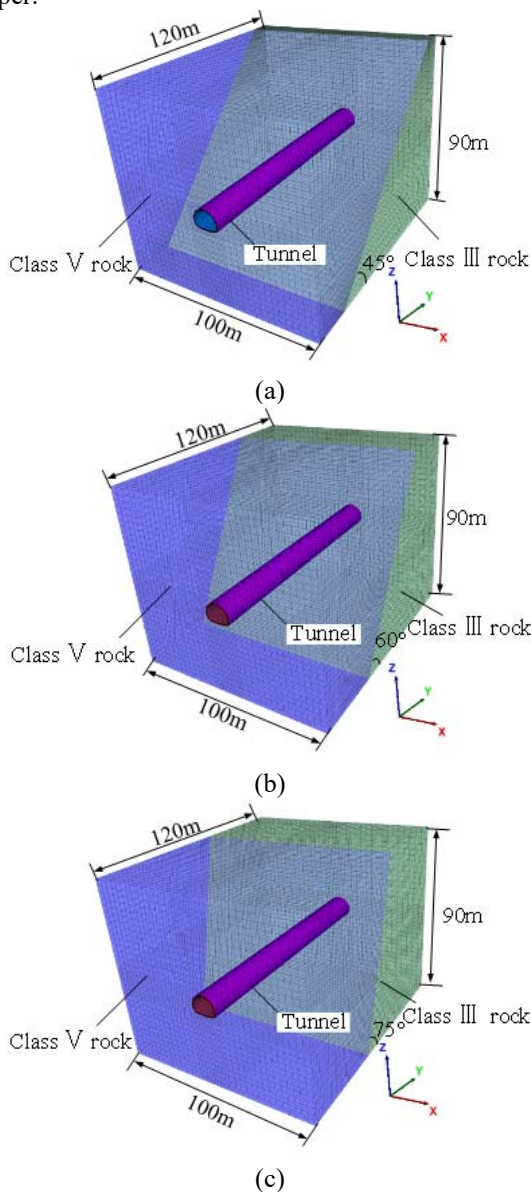


Figure (3): Numerical model; (a) 45°; (b) 60°; (c)75°

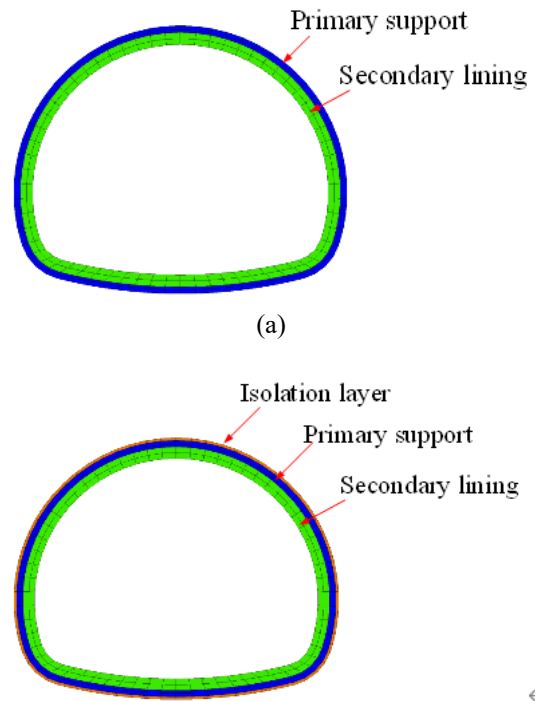


Figure (4): Tunnel support; (a) control models without seismic measures; (2) study models with isolation layer

Table 1. Test cases

Test cases	The dip angle of the interface	Description
1	45°	Non-seismic measures
2		Tunnel with isolation layer
3	60°	Non-seismic measures
4		Tunnel with isolation layer
5	75°	Non-seismic measures
6		Tunnel with isolation layer

Material Parameters

The elastic modulus, Poisson's ratio, friction angle and cohesion of the surrounding rock are measured by the triaxial compression test. Through the elastic modulus and Poisson's ratio tests, the elastic modulus and Poisson's ratio of concrete are tested. Table 2 lists the necessary parameters of the materials in the numerical simulation.

Table 2. Parameters of materials

Name	Density (kg/m ³)	Modulus of elasticity/GPa	Poisson's ratio	Friction angle (°)	Cohesion (MPa)
Moderately weathered granite (class III) ^a	2000.0	15.0	0.3	45.0	1.0
Strongly weathered granulite (class V) ^a	2400.0	2.0	0.4	25.0	0.2
Bedrock (class II) ^a	2500.0	20.0	0.2	50.0	1.5
C20 shotcrete ^b	2200.0	25.0	0.2	/	/
C25 modeled concrete ^b	2550.0	28.0	0.2	/	/
Sponge rubber plate	1000.0	0.3	0.5	0.5	5.0

^a class in code for design of the road tunnel (Ministry of Transport of the People's Republic of China, 2004).

^b intensity class in code for design of concrete structures (MOHURD, 2011).

Dynamic Calculation

In FLAC3D dynamic calculation, the dynamic load could be directly applied to boundary or internal nodes through the acceleration time history, velocity time history, stress and stress time history, ... etc. The seismic acceleration time history measured by Wolong station in 2008 Wenchuan earthquake is used as the dynamic load in this paper, since its typical characteristics could reflect the real seismic wave conditions of the tunnel site area. The original wave has been filtered and baseline

corrected by professional seismic wave processing software, so as to reduce the influence of grid size on seismic waves (Sandoval and Bobet, 2020). The duration of the processed seismic acceleration wave is 15s, the acquisition interval is 0.01s and it has 85% of the energy of the original wave, as shown in Figure 5. The seismic wave propagates upward from the bedrock at the bottom of the model and the horizontal, vertical and longitudinal seismic waves correspond to the x, y and z directions of the model.

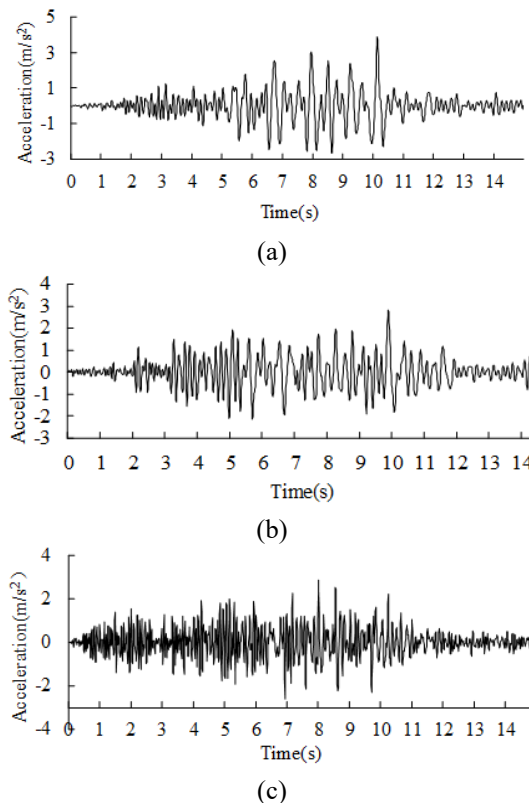


Figure (5): Time history of dynamic load: (a) horizontal; (b) vertical; (c) longitudinal

The local damping of FLAC3D is independent of the frequency and does not need to estimate the natural frequency of the simulated system, which could be able to accurately reproduce the damping of natural system under the seismic action. Therefore, the local damping with a coefficient of 0.1571 is adopted in the numerical model. In the dynamic calculation, relevant boundary conditions must be used to reduce the reflection of dynamic load on the model boundary after input and absorb the reflected energy. The free field boundary in FLAC3D is used for the seismic calculation, which can show the effect similar to the infinite field model, so that the seismic wave will not be distorted or reflected in the transmission process. The relevant tool of ANSYS APDL is used to mesh the numerical model. The element shape of the numerical model is a brick consisting of 8 grid points, which is the most suitable mesh type for the numerical example. Considering the influence of grid size on the calculation time and the accuracy of the results, the longitudinal, transverse and vertical mesh side of the numerical model is 2.5m, 4m and 4m, respectively. The mesh size of tunnel hole and linings is about 1m wide and 0.25m thick.

Monitoring System

The history command in FLAC can dynamically monitor the displacement, stress and strain of each element and node during the dynamic analysis and output the time history curve at the end of calculation. Nine monitoring sections named from S1 to S9 are set in the longitudinal direction of the tunnel to collect the displacement, principal stress, axis force and bending moment data of the tunnel structure in the earthquake. From S1 to S9, the range of soft rock increases, while the range of hard rock decreases. Fig.6(a) plots the monitoring sections of the tunnel. In each section, eight measuring points (i.e., invert arch, right arch foot, right side wall, right spandrel, vault, left spandrel, left side wall and left arch foot) are set to collect the dynamic data of the internal force and stress of the tunnel under different test conditions, as shown in Fig.6 (b).

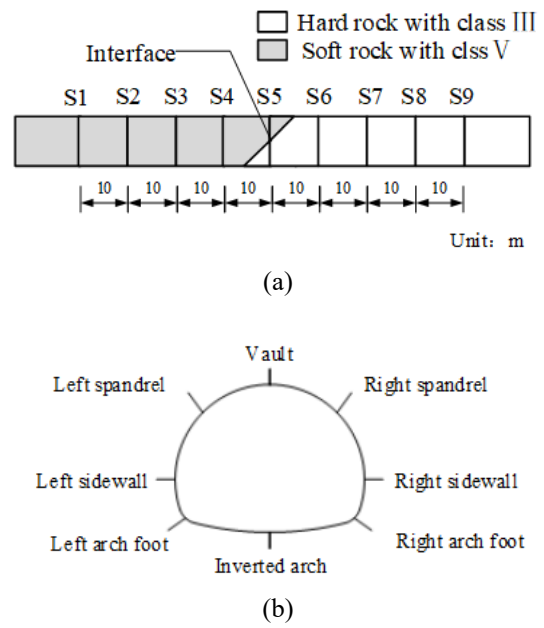


Figure (6): Monitoring system; (a) monitoring sections; (b) measuring points

Internal Force Calculation

Although FLAC3D can accurately simulate the dynamic response of the tunnel in earthquake, it can only analyze the deformation, stress and strain of the structure, but cannot directly obtain the axial force and the bending moment of the structure. In view of this, the calculation of axial force and bending moment of lining structure (Fig. 7) is derived as in Equations (1) and (2).

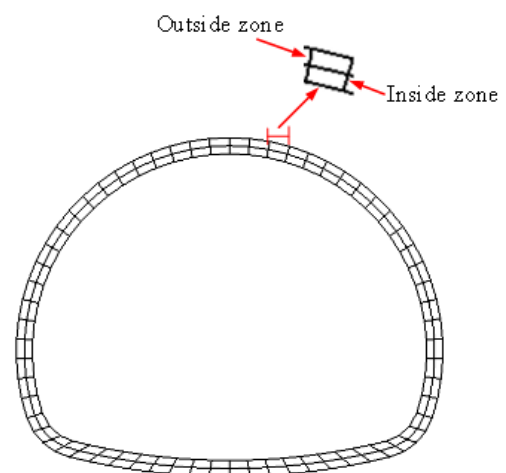


Figure (7): Lining models

$$N = \frac{E(\sigma_1 + \sigma_2)bh}{2} \quad (1)$$

$$M = \frac{E(\sigma_1 - \sigma_2)bh^2}{12} \quad (2)$$

where N is the axis force, M is the bending moment, E is the elastic modulus, σ_1 is internal stress of lining which is calculated by Equation (3), σ_2 is the external stress of lining which is calculated by Equation (4), b is the width of the tunnel section and h is the thickness of the tunnel section.

$$\sigma_1 = \zeta(\sigma_{n1} + \sigma_{n2}) + \frac{\zeta(\sigma_{n1} + \sigma_{n2})}{\xi} \quad (3)$$

$$\sigma_2 = \zeta(\sigma_{n1} + \sigma_{n2}) - \frac{\zeta(\sigma_{n1} + \sigma_{n2})}{\xi} \quad (4)$$

where ζ is the reciprocal of lining zone layers, σ_{n1} is the normal stress of the internal grid, σ_{n2} is the normal stress of the external zone and σ_{n1}/σ_{n2} is derived by Equation (5).

$$\sigma_n = \sigma_x \cos^2(-\alpha) + \sigma_y \sin^2(-\alpha) + \sigma_{xy} \sin(-2\alpha) \quad (5)$$

where α is the angle between the line of centroid of inner and outer elements and vertical direction, which is calculated by Equation(6); (x_1, y_1) and (x_2, y_2) are the centroid coordinates of the inner and outer zones, respectively.

$$\alpha = \arctan\left(\frac{x_2 - x_1}{y_2 - y_1}\right) \quad (6)$$

In this paper, the safety factor from the Code for Design of Road Tunnel (Ministry of Transport of the People's Republic of China, 2004) is used to estimate the stability and the safety of the tunnel, which are calculated by Equations (7) and (8). The larger the safety factor, the safer the structure.

$$KN \leq \varphi\delta R_a bh \quad (7)$$

$$KN \leq \varphi \frac{1.75 R_t bh}{\frac{6e_0}{h} - 1} \quad (8)$$

where K is the safety factor, φ is the longitudinal bending coefficient, δ is the influence coefficient of axial force eccentricity, R_a is the ultimate compressive strength of concrete, R_t is the ultimate tensile strength of concrete and e_0 is the eccentricity of the section.

RESULTS AND ANALYSIS

Maximum Principal Response

In the dynamic calculation, the principal stress of each measuring point is dynamically monitored and the time history curve is shown in Fig. 8 (taking the invert arch of S5 section in Case 4 as an example for illustrating). The peak of the maximum principal stress during the seismic excitation was extracted from the time history wave, as shown in Fig. 9.

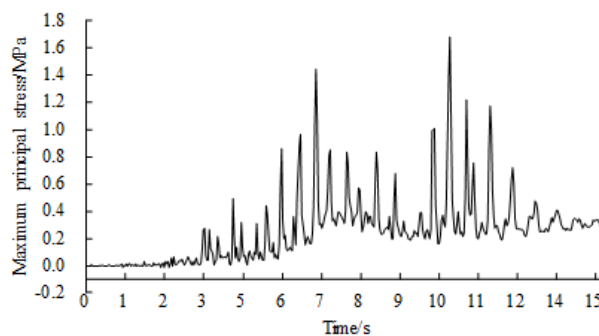
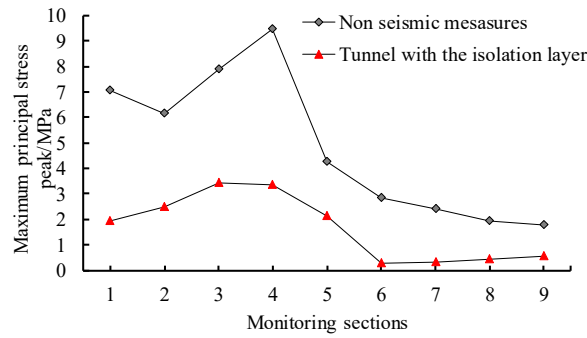
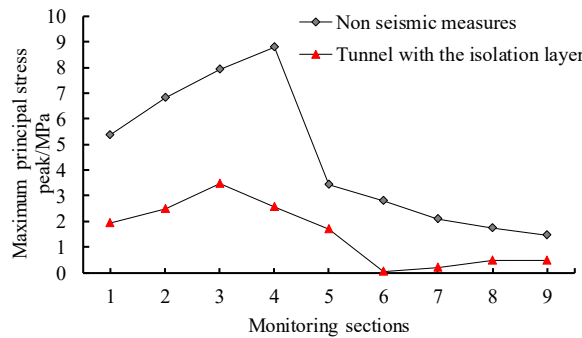


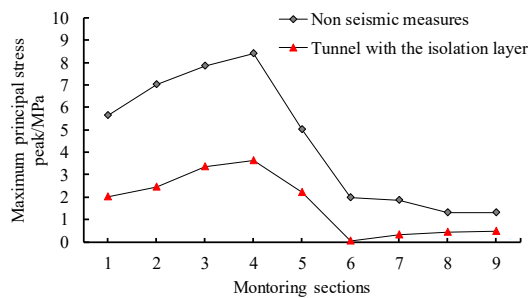
Figure (8): Time history curve of the maximum principal stress



(a)



(b)



(c)

Figure (9): Maximum principal peak; (a) 45°; (b) 60°; (c) 75°

In the longitudinal direction of the tunnel, the maximum principal stress of the tunnel in soft rock is much higher than that in hard rock, which indicates that the structure in the soft rock may experience stronger seismic motion and suffer more serious damages than that in the hard rock, corresponding to the tunnel seismic investigation of recent strong earthquakes. After the isolation layer is applied into the tunnel lining, the maximum principal stresses of the three study models significantly decreased, which shows that the isolation layer has a remarkable blocking effect on the seismic force. Compared with the tunnel without any seismic

measures, the reduction percentage of the maximum principal stress peak of the structure with the isolation layer is shown in Table 3. The results show that the peak of the maximum principal stress decreases by 50.23%-89.96% when the dip angle of the soft-hard interface is 45°, 51.26%-98.95% when the dip angle of the junction is 60° and 55.98%-97.39% when the angle of the junction is 75°. The influence of isolation layer on the maximum principal stress peak value of the structure at the interface angles of 45°, 60° and 75° is basically similar. The reduction in maximum principal stress peak in the soft rock is much larger than that in the hard rock.

The peak values of the reduction percentage in the three study models all appear in S6 section, while the minimum of the reduction occurs in S5 section.

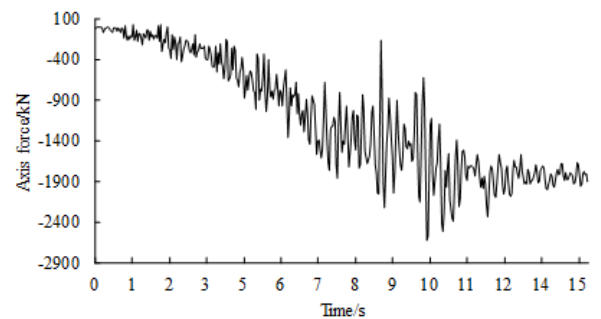
Table 3. Reduction of the maximum principal stress

Monitoring sections	45°	60°	75°
1	72.66%	63.69%	64.54%
2	59.90%	63.84%	64.91%
3	56.47%	56.31%	57.14%
4	64.69%	70.88%	57.07%
5	50.23%	51.16%	55.98%
6	89.96%	98.95%	97.39%
7	87.11%	89.71%	82.55%
8	77.72%	73.31%	66.43%
9	69.21%	67.35%	63.41%

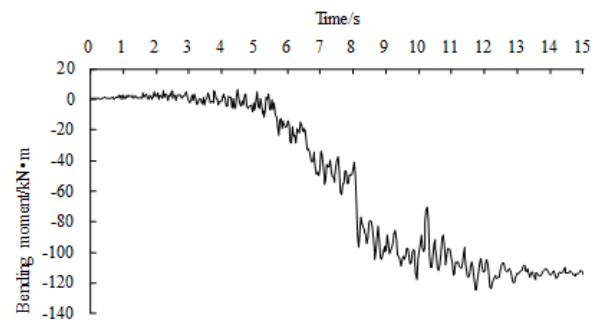
Internal Force Response

Fig. 10 plots the time history curves of the axis forces, the bending moment and the safety factor, where the vault point of section 3 in Case 4 is chosen as an example for illustrating. In this paper, the minimum safety factor of measuring points is used as a criterion to judge the safety of a monitoring section, where the larger the minimum safety factor is, the better is the structural safety. The minimum safety factor of the measuring points could be extracted from the time history curve and the minimum safety factor values over monitoring sections of six test cases are shown in Fig. 11. Overall, the minimum safety factor is positively correlated with the proportion of hard rock; that is, the larger the hard rock range in the tunnel surrounding, the larger the structural safety factor. It can be concluded that the safety of tunnel structure is related to the proportion of soft rock in surrounding rock and the tunnel with the large proportion of soft rock suffers serious damage in strong earthquakes. The isolation layer blocks the transmission of seismic force to the tunnel lining, so that the safety factor of the tunnel structure is also improved. Table 4 lists the ant seismic effect of the safety factor caused by the application of the isolation layer, i.e., the increase percentage of the minimum safety factor in the study model relative to the control model. The seismic effect of the isolation layer is 2.45%-121.67% when the

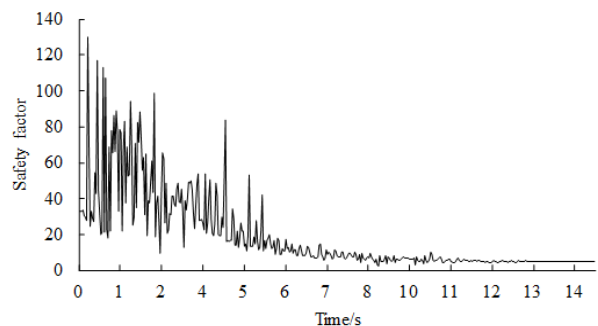
dip angle of soft and hard rock interface is 45°, 13.19%-66.98% when the dip angle of the interface is 60° and 4.60%-131.83% when the dip angle is 75°. For the monitoring section intersecting with soft-hard interface(S5), the seismic effect is weakest along the tunnel longitudinal direction, which is 2.45%, 10.76% and 5.15%, respectively at the dip angle of 45°, 60° and 75°. The application of the isolation layer significantly increases the safety of the tunnel crossing the soft and hard rock junction, except for the structure located at the soft-hard rock interface. It is suggested to adopt both isolation measures and structure reinforcements at the structure intersecting the soft and hard rock interface.



(a)

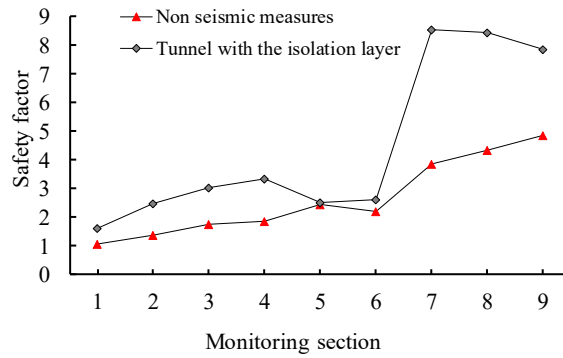


(b)

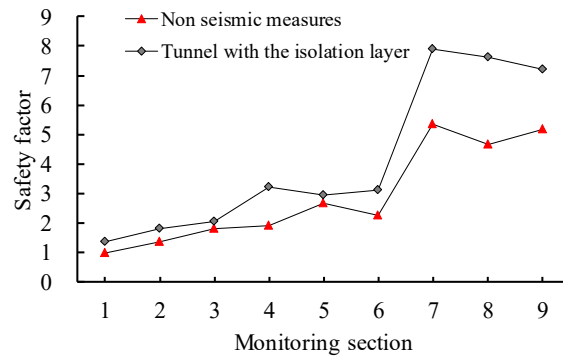


(c)

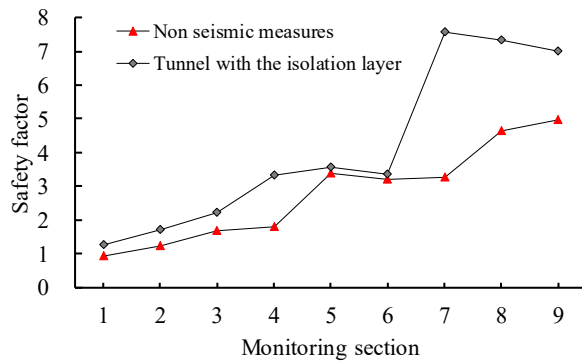
Figure (10): Time history of the internal force; (a) axis force; (b) bending moment; (c) safety factor



(a)



(b)



(c)

Figure (11): Minimum safety factor; (a) 45°; (b) 60°; (c) 75°

Table 4. Seismic effect of the isolation layer

Monitoring sections	45°	60°	75°
1	51.85%	35.65%	34.50%
2	81.36%	32.35%	38.93%
3	73.88%	13.19%	31.43%
4	79.26%	66.98%	83.80%
5	2.45%	10.76%	5.15%
6	19.23%	36.90%	4.60%
7	121.67%	47.23%	131.83%
8	94.64%	63.16%	57.98%
9	61.49%	39.57%	41.18%

DISCUSSION AND CONCLUSIONS

In view of the severe seismic damage that happened at the tunnel soft and hard rock junction, this paper aims to study the seismic effect of the isolation layer in the junction. Firstly, six finite difference models considering the modified waves, the mechanical damping, the dip angle of soft-hard rock interface and the isolation layer are established to investigate the seismic response of the tunnels intersecting with different dip angles. Then, applying the isolation layer into the tunnel models, we have studied the seismic effect of the isolation in the soft and hard rock junction. Finally, through the comparison of the seismic effect of the dip angle at 45°, 60° and 75°, the dip angle effect of the soft and hard rock on the seismic behavior of the isolation layer is obtained. Though the type of the seismic wave, the material of the isolation layer and the excitation direction have not been considered in this paper, as these factors will not directly affect the isolation performance of the layer except for introducing some new irrelevant variables. Some key findings are

listed below:

- (1) The seismic safety of the tunnel located at the soft-hard rock junction is related to the proportion of soft and hard rock materials. The larger the proportion of soft rock is, the more vulnerable is the tunnel structure to seismic waves.
- (2) After applying the isolation layer in tunnel structures, the maximum principal stress has been decreased by 50.23%-89.96%, 51.16%-98.95% and 55.98%-97.39%, respectively, at the dip angle of 45°, 60° and 75°. The seismic effect of the isolation layer of the soft-hard rock interface of 45°, 60° and 75° is 2.45%-121.67%, 13.19%-66.98% and 4.60%-131.83%, respectively.
- (3) The application of the isolation layer could remarkably increase the safety of the tunnel crossing the soft and hard rock junction, except for the structure located at the soft-hard rock interface. It is suggested to adopt both isolation measures and structure reinforcements at the structure intersecting the soft and hard rock interface.

REFERENCES

- Chen, Z., Liang, S., Shen, H., and He, C. (2018). "Dynamic centrifuge tests on effects of isolation layer and cross-section dimensions on shield tunnels". *Soil Dynamics and Earthquake Engineering*, 109, 173-187; doi:<https://doi.org/10.1016/j.soildyn.2018.03.002>
- Cui, G., Wang, M., Lin, G., Zhang, W., and Wang, W. (2011). "Study of the earthquake damage mechanism and a seismic countermeasure of a highway tunnel portal section in the Wenchuan seismic disaster area". *Xiandai Suidao Jishu* 48, 6-10; doi:10.13807/j.cnki.mtt.2011.06.004
- Dowding, C.H., and Rozen, A. (1978). "Damage to rock tunnels from earthquake shaking". *ASCE J. Geotech, Eng. Div.*, 104, 175-191.
- Esfeh, P.K., and Kaynia, A.M. (2020). "Earthquake response of monopiles and caissons for offshore wind turbines founded in liquefiable soil". *Soil Dynamics and Earthquake Engineering*, 136; doi: <https://doi.org/10.1016/j.soildyn.2020.106213>
- Hashash, Y.M.A., Hook, J.J., Schmidt, B., and Chiang, Yao J. (2001). "Seismic design and analysis of underground structures". *Tunnelling and Underground Space Technology*, 16, 247-293; doi:[https://doi.org/10.1016/S0886-7798\(01\)00051-7](https://doi.org/10.1016/S0886-7798(01)00051-7)
- Hassan, R.F., Risan, H.K., and Hussein, H.A. (2021). "Seismic behavior of reinforced concrete rectangular water tank on grade with wall opening". *Jordan Journal of Civil Engineering*, 15, 12-29.
- He, J., Chen, W., Zhao, W., Huang, S., and Yao, Y. (2016). "Numerical test on polystyrene tunnel seismic-isolation material". *Polish Journal of Chemical Technology*, 18, 122; doi:<https://doi.org/10.1515/pjct-2016-0058>
- Ismail, S., Kaddah, F., and Raphael, W. (2020). "Seismic soil-structure interaction response of midrise concrete structures on silty sandy soil". *Jordan Journal of Civil Engineering*, 14, 117-135.
- Itasca Consulting Group, Inc. (2015). "FLAC3D-fast Lagrangian analysis of continua in 3 dimensions". Ver. 5.0 user's manual. Itasca Consulting Group, Inc., Minneapolis.

- Jamshidi Avanaki, M., Hoseini, A., Vahdani, S., de Santos, C., and de la Fuente, A. (2018). "Seismic fragility curves for vulnerability assessment of steel fiber-reinforced concrete segmental tunnel linings". *Tunnelling and Underground Space Technology*, 78, 259-274; doi:<https://doi.org/10.1016/j.tust.2018.04.032>
- Kim, D.S., and Konagai, K. (2000). "Seismic isolation effect of a tunnel covered with coating material". *Tunnelling and Underground Space Technology*, 15, 437-443; doi:[https://doi.org/10.1016/S0886-7798\(01\)00012-8](https://doi.org/10.1016/S0886-7798(01)00012-8)
- Konagai, K., and Kim, D.S. (2001). "Simple evaluation of the effect of seismic isolation by covering a tunnel with a thin flexible material". *Soil Dynamics & Earthquake Engineering*, 21, 287-295.
- Konagai, K., Takatsu, S., Kanai, T., Fujita, T., Ikeda, T., and Johansson, J. (2009). "Kizawa tunnel cracked on 23 October 2004 Mid-Niigata earthquake: An example of earthquake-induced damage to tunnels in active-folding zones". *Soil Dynamics and Earthquake Engineering*, 29, 394-403; doi: <https://doi.org/10.1016/j.soildyn.2008.04.002>
- Li, T. (2012). "Damage to mountain tunnels related to the Wenchuan earthquake and some suggestions for a seismic tunnel construction". *Bulletin of Engineering Geology & the Environment*, 71, 297-308; doi:<https://doi.org/10.1007/s10064-011-0367-6>
- Ma, S., Chen, W., and Zhao, W. (2019). "Mechanical properties and associated seismic isolation effects of foamed concrete layer in rock tunnel". *Journal of Rock Mechanics and Geotechnical Engineering*, 11, 159-171; doi:<https://doi.org/10.1016/j.jrmge.2018.06.006>
- Marti, J., and Cundall, P. (1982). "Mixed discretization procedure for accurate modeling of plastic collapse". *International Journal for Numerical and Analytical Methods in Geomechanics*, 6, 129-139; doi:<https://doi.org/10.1002/nag.1610060109>
- Mayoral, J.M., and Mosqueda, G. (2020). "Seismic interaction of tunnel-building systems on soft clay Soil". *Dynamics and Earthquake Engineering*, 139, 106419; doi: <https://doi.org/10.1016/j.soildyn.2020.106419>
- Ministry of Transport of the People's Republic of China. (2004). "Code for design of road tunnel: TG D70-2004". China Communication Publishing & Media Management Co., Ltd., Beijing, China.
- MOHURD. (2011). "Code for design of concrete structures". China Construction Industry Press, Beijing.
- Patil, M., Choudhury, D., Ranjith, P.G., and Zhao, J. (2018). "Behavior of shallow tunnel in soft soil under seismic conditions". *Tunnelling and Underground Space Technology*, 82, 30-38; doi:<https://doi.org/10.1016/j.tust.2018.04.040>
- Rinaldi, A.P., and Urpi, L. (2020). "Fault reactivation induced by tunneling activity in clay material: Hints from numerical modeling". *Tunnelling and Underground Space Technology*, 102, 9; doi: <https://doi.org/10.1016/j.tust.2020.103453>
- Sandoval, E., and Bobet, A. (2020). "Effect of input frequency on the seismic response of deep circular tunnels". *Soil Dynamics and Earthquake Engineering*, 139, 106421; doi:<https://doi.org/10.1016/j.soildyn.2020.106421>
- Shimamura, S., Kasai, H., and Haruumi, M. (1999). "Seismic isolation effect for a tunnel with a soft isolation layer". *Structural Engineering Earthquake Engineering*, 16, 143s-154s.
- Suzuki, T., Takatori, I., Okada, I., and Hagiwara, R. (2002). "New seismic isolation design for urban tunnels in consideration of slip and its application to an actual shield-driven tunnel". In: AITES-ITA Downunder 2002: 28th ITA General Assembly and World Tunnel Congress, Sydney, Australia, 2-8 March 2002: Modern Tunnels-Challenges and Solutions, Japan, Institution of Engineers, 708.
- Tsinidis, G. et al. (2020). "Seismic behaviour of tunnels: From experiments to analysis". *Tunnelling and Underground Space Technology*, 99, 103334; doi:<https://doi.org/10.1016/j.tust.2020.103334>
- Wang, W.L., Wang, T.T., Su, J.J., Lin, C.H., Seng, C.R., and Huang, T.H. (2001). "Assessment of damage in mountain tunnels due to the Taiwan Chi-Chi earthquake". *Tunnelling and Underground Space Technology*, 16, 133-150; doi: [https://doi.org/10.1016/S0886-7798\(01\)00047-5](https://doi.org/10.1016/S0886-7798(01)00047-5)
- Zhao, W., Chen, W., and Yang, D. (2018). "Interaction between strengthening and isolation layers for tunnels in rock subjected to SH waves". *Tunnelling and Underground Space Technology*, 79, 121-133; doi:10.1016/j.tust.2018.05.012.